Journal of Ovarian Research

RESEARCH

Open Access

Downregulation of FASN in granulosa cells and its impact on ovulatory dysfunction in PCOS

Zhaoping Tan[1,2,3], Tiancheng Wu[1,2,3], Mei Wang[1,2,3], Liang Chen[1,2,3], Yating Li[1,2,3], Ming Zhang[1], Yuanzhen Zhang[4,5*] and Lili Sun[2,4*]

Abstract

Background Polycystic ovary syndrome (PCOS) is a complicated endocrinological and anovulatory disorder in women. Mice exposed to dihydrotestosterone (DHT) exhibit a PCOS-like phenotype characterized by abnormal steroid hormone production and ovulation dysfunction. The present investigation aims to identify overlapping genes expressed in PCOS patients and a PCOS mouse model induced by DHT and to examine the function of key genes fatty acid synthase (FASN) in hormone production and ovulation dysfunction.

Results We examined 5 datasets of high-throughput mRNA transcription from the Gene Expression Omnibus (GEO) database, including 4 datasets from individuals with PCOS and 1 dataset from a DHT-induced mouse model. GO and KEGG enrichment analyses revealed these differentially expressed genes (DEGs) are primarily involved in ovarian steroidogenesis and fatty acid metabolism. The PPI network identified 12 hub genes. qRT-PCR verification in human granulosa cells showed differential expression of FASN, SCARB1, FABP5, RIMS2, and RAPGEF4 in PCOS patients ($p < 0.05$). FASN was downregulated in the granulosa cells (GCs) of PCOS patients ($p < 0.05$). FASN depletion reduced KGN cell proliferation ($p < 0.001$), decreased progesterone secretion ($p < 0.05$), and increased estradiol secretion ($p < 0.05$). Downregulation of FASN inhibited ovulation by suppressing ERK1/2 phosphorylation and the expression of C/EBPα and C/EBPβ. Lentivirus-mediated FASN downregulation in rat ovaries for one and four weeks impaired the super ovulatory response, reducing oocyte retrieval, estrous cycle, secretion of estrogen and progesterone, and luteinization.

Conclusions Our results provide new insights into PCOS pathogenesis and suggest that FASN could be a promising target for treating abnormal steroid hormone production and impaired ovulation in PCOS.

Keywords Polycystic ovary syndrome, FASN, Bioinformatic analysis, Ovulatory dysfunction

*Correspondence:
Yuanzhen Zhang
zhangyuanzhen@whu.edu.cn
Lili Sun
lilysun827@163.com
[1] Center for Reproductive Medicine, Zhongnan Hospital of Wuhan University, Wuhan, Hubei, People's Republic of China
[2] Department of Gynecological Oncology, Zhongnan Hospital of Wuhan University, Wuhan, Hubei 430071, People's Republic of China
[3] Clinical Medicine Research Center of Prenatal Diagnosis and Birth Health in Hubei Province, Wuhan, Hubei, People's Republic of China
[4] Wuhan Clinical Research Center for Reproductive Science and Birth Health, Wuhan, Hubei, People's Republic of China
[5] Department of Obstetrics and Gynecology, Zhongnan Hospital of Wuhan University, Wuhan, Hubei 430071, People's Republic of China

Background

Polycystic ovary syndrome (PCOS), with an estimated occurrence rate ranging from 11 to 13%, affects a substantial number of women's intricate hormonal and metabolic systems in their reproductive years [1, 2]. The condition is specified by infertility caused by absence of ovulation, hormonal irregularities [3]. PCOS is responsible for over 75% of anovulatory infertility cases, resulting from follicular halt and ovulatory dysfunction [4]. But the exact mechanisms responsible for abnormal follicular growth and anovulation in people with PCOS are still not fully understood.

Among the various cell types implicated in PCOS pathogenesis, granulosa cells (GCs) have emerged as significant contributors [5]. Located around the oocyte, GCs providing oocytes with nutrition along with growth regulators throughout their maturation process [6] and regulate steroid hormone levels [2], which are tightly controlled during oocyte maturation [7]. Dysregulation of steroid hormone levels in GCs and the lipid metabolism of GCs play a crucial part in PCOS pathophysiology.

Activation of Luteinizing Hormone/Chorionic Gonadotropin (LH/CG) receptors by LH in the mural GCs of big follicles triggers a signal that transmits the cells of cumulus and oocytes via paracrine and autonomous signals. This signal causes meiosis to resume, cumulus cells to expand, and the cumulus-oocyte complex to rupture, resulting in the release of a fertile egg capable of fertilization [8]. Throughout this process, epidermal growth factor receptor (EGFR)/extracellular signal-regulated kinase (ERK 1/2) signaling pathway and ERK1/2 phosphorylation play pivotal roles [9]. Forskolin possesses the capacity to induce EGFR transactivation in granulosa cells. ERK1/2 activated downstream mediator C/EBPβ (CCAAT/Enhancer-binding protein β) [9, 10]. Therefore, the LH-regulated in vivo signaling pathway involving ERK1/2 and C/EBPβ governs ovulation and luteinization-related events [9].

Hyperandrogenic mice models induced with dihydrotestosterone (DHT) are widely used in current experiments because they exhibit a phenotype resembling PCOS. These models are exhibit by menstrual abnormalities, multiple ovarian cysts, insulin resistance, increased body weight, adipocyte hypertrophy, and hypercholesterolemia [11].

Identification of common differentiation genes between human PCOS and DHT model mice is crucial for uncovering the causes of anovulation in PCOS. As shown in Fig. 1, this study aims to identify common differentiation genes between granulosa cells derived from

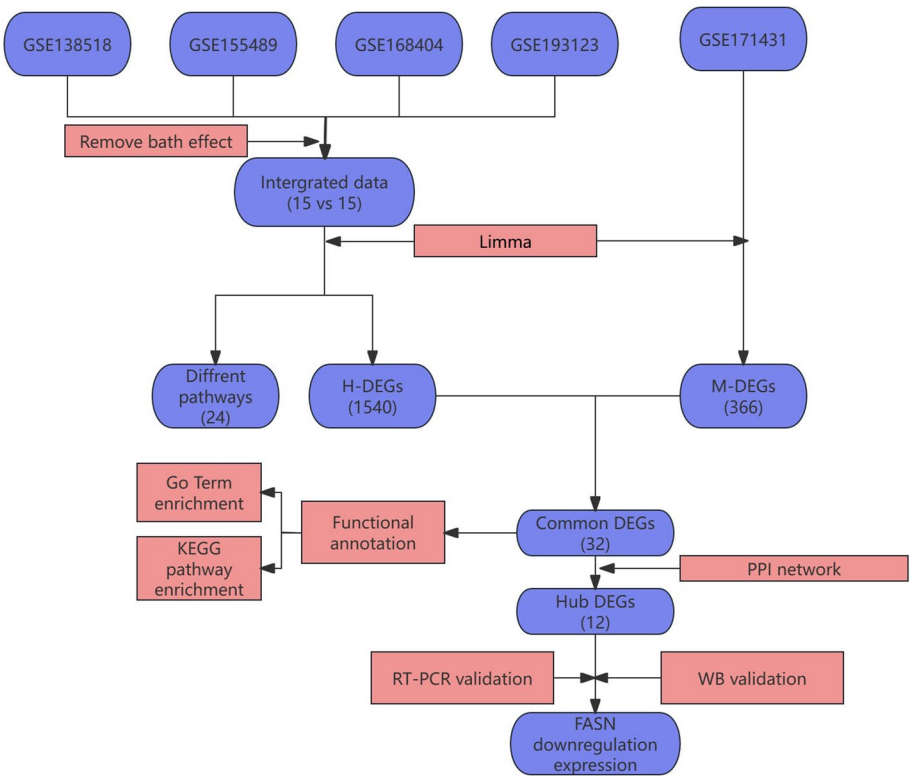

Fig. 1 Flow chart

patients with PCOS and ovaries from DHT-induced mice and validate these results in human GCs. By validating the role of these genes in granulosa cell proliferation, hormone secretion and especially ovulation dysfunction, this approach will help identify new marker molecules for PCOS and offer new perspectives for the further development of innovative therapies for anovulatory infertility with the aim of helping people with PCOS.

Methods

Microarray data

We obtained PCOS datasets from the Gene Expression Omnibus (GEO) database(http://ncbi.nlm.nih.gov/geo/) using high-throughput methods. We employed samples of ovarian granulosa cells as target organs. We obtained several GEO series, comprising four transcriptome RNA sequencing datasets (GSE138518, GSE155489, GSE168404, GSE193123). The data set consisted of expression profiles from 15 individuals diagnosed with PCOS and 15 tuber factors individuals serving as controls. We also chose a DHT-induced mouse database to provide additional validation of the importance and precision of our results, GSE171431: 6 samples of ovarian DHT-treated mice($n=3$) and ovaries of control mice($n=3$).

Data pre-processing

We obtained the representation matrix from the four transcriptome RNA sequencing datasets, the data integration and pre-processing were performed utilizing the Sangerbox platform [12]. Firstly, genes with missing values (NA) exceeding 50% were eliminated, as well as samples with missing values exceeding 50%. In addition, we use the R package impute function to complete missing values and set 10 of neighbors to K to complete missing data. The data were then further normalized using the median. We employed the "inSilicoMerging" R package for data merging and applied a Bayesian approach to adjust for batch effects in the microarray expression data.

Detection and functional enrichment analysis of DEGs

Data preprocessing was performed in the R programming environment (version 4.2.2). Specifically, the "limma" package was used to generate differentially expressed genes (DEGs) between the PCOS and control patients [13]. DEGs were determined using a threshold of $|\log2\ FC|>1$ and $p<0.05$. The packages "complexheatmap" and "ggplot2" were used to create heatmaps and volcano plots. A Venn diagram was then used to identify overlapping DEGs between human samples and DHT-induced mouse models from the GSE171431 dataset (http://www.bioinformatics.com.cn/static/others/jvenn/example.html).

Using the SangerBox platform, we conducted Gene Ontology (GO) and Kyoto Encyclopedia of Genes and Genomes (KEGG) annotation analyses to identify the biological functions of the DEGs [12]. We used the R software package "org.Hs.eg.db" (version 3.1.0) to assign genetic information to the reference group set based on their GO annotations. The enrichment analysis was carried out utilizing the R software package "clusterProfiler" (version 3.14.3), by setting the minimum gene set size to 5 and the maximum gene set size to 5000 and $p<0.05$ was considered statistically significant.

Identification of gene clusters and construction of protein–protein interaction network

Utilizing the STRING database (https://string-db.org/), we generated a protein–protein interaction network (PPI), then the results were loaded into the Cytoscape v3.9.1 software for the purpose of identifying key nodes. The PPI network diagram was obtained via STRING's online database and the CytoHubba plugin was employed to identify key genes important for molecular interactions within the network. A PPI network was created using DEGs with a confidence value of 0.4, proteins not linked to other proteins were removed.

Human ovarian granulosa cell collection and ethics statement

Human ovarian granulosa cell samples were obtained from patients undergoing in vitro fertilization (IVF) treatment at the Reproductive Medicine Center of Zhongnan Hospital, Wuhan University. The whole experiment was reviewed by the ethics committee (NO.2021136 K). Patients in the PCOS group were selected in accordance with the Rotterdam diagnostic criteria [1, 3]. PCOS diagnosis necessitates the presence of a minimum of two of the following criteria: a) Infrequent or absent ovulation; b) Manifestations of excessive male hormone levels, either in physical symptoms or laboratory tests; and c) Presence of many cysts on the ovaries. The standards used to choose control women were as follows: a) Menstrual cycles occurring at regular intervals of 25–35 days, b) Absence of any anomalies in the endocrine system, and c) Normal appearance of the ovaries as confirmed by ultrasound imaging.We recruited a total of 40 IVF patients, including 20 with PCOS and 20 in the control group with tubal or male factor infertility. From this cohort, we extracted total RNA from 11 PCOS patients and 11 controls, and proteins from 9 PCOS patients and 9 controls.

Cell line culture and treatment

The ovarian granulosa cell lines KGN and 293T were stored in the central laboratory of Zhongnan Hospital.

KGN cells were cultured in DMEM/F12 medium (Biological Industries, USA) containing 10% fetal bovine serum (Biological Industries, USA) and 100 U/ml penicillin/streptomycin (Biological Industries, USA) at 37 °C in a humidified atmosphere with 5% CO2.The 293T cells were cultured in high glucose DMEM (Biological Industries, USA) supplemented with 10% fetal bovine serum (Biological Industries, USA) and 100 U/ml penicillin/streptomycin (Biological Industries, USA). Cells were normally maintained in an incubator at 37 °C and 5% CO_2. To imitate the impact of LH surge and activate the ERK signaling pathway in KGN cells, forskolin (FSK, MedChemExpress, Shanghai, China) was applied at a dose of 10 mM. To reduce ERK signaling, cells were first exposed to a 10 mM concentration of U0126, a MEK1/2 inhibitor from MedChemExpress in Shanghai, China, for 1 h. This was followed by a 4-h treatment with FSK [10, 14].

Packaging and titer determination of the downregulated FASN lentivirus

293T cells with robust growth were selected and seeded into 10 cm culture dishes, then maintained in an incubator at 37 °C and 5% CO_2 until reaching a cell density of 70%−80% for transfection. FASN group (transfected with pLVX-shFASN-ZsGreen-T2A-Puro, Pmd2.G, PSPAX2) (Wuhan Qijing Biological Technology Co., Ltd) and control group (transfected with pLVX-NC-ZsGreen-T2A-Puro, Pmd2.G, PSPAX2) (Wuhan Qijing Biological Technology Co., Ltd) were established. Following the instructions of Lipofectamine 3000 (Invitrogen), the transfection reagent was introduced into the 293T cells. After 6 h of transfection, complete high high glucose DMEM medium was to replace the Opti-MEM medium. The supernatant containing lentiviral particles was collected after continuous culture for 48 h and filtered through a 0.45um filter to obtain virus solution. The virus solution was diluted by factors of ten from 10^1 to10^6 before inoculation into new batches of 293T cells. After culturing at 37 °C and 5% CO_2 for 72 h, green fluorescent cells were counted under fluorescence microscope to calculate viral titer.

Establishment of KGN cells stably transfected with FASN knockdown and control lentiviral vectors

KGN cells were grown until 70–80% confluency was reached, subsequently, the cells were transfected with lentivirus carrying human Fatty acid synthase (FASN) down-regulation vectors (sh-FASN) or control vectors (sh-NC) at a virus titer of $1*10^8$ TU/ml. Two days later, the cells were subjected to puromycin treatment at a concentration of 2 mg/ml. After 7 days, dead cells no longer appeared. Cell lines that were stable were analyzed for FASN expression by qRT-PCR and immunoblotting.

RNA isolation and quantitative real-time PCR (qRT-PCR)

Human follicular granulosa cells and KGN were subjected to RNA extraction using Aidlab RNA extraction kit RN0302. A one microgram amount of RNA was subjected to reverse transcription using the Vazyme cDNA synthesis kit (R2-12–01). For quantitative real-time PCR (qRT-PCR), each reaction contained the overall volume of 10μL, consisting of 2 ChamQ SYBR qPCR Master Mix (5μL), forward and reverse primers (1μL each), and cDNA (1μL) and distilled water (3μL) using the primers specified in Supplementary Table 1. The PCR system uses CFX96 equipment manufactured by Bio-Rad Laboratories.

Extraction of protein and analysis via Western blotting

The cells were harvested and then the entire cell protein extract was separated from them. Protein concentrations were measured using a BCA Protein Assay Kit (P0010, Beyotime, China). The denatured protein was divided into equal amounts and then subjected to electrophoresis using 7.5% SDS–polyacrylamide gels. Subsequently, the protein was transferred to polyvinyl difluoride membranes (Millipore, Billerica, USA). The samples were first treated using blocking substance for 1 h. They were then incubated overnight at 4 °C with the following primary antibodies: polyclonal rabbit anti-FASN (3180; 1:1,000 dilution; Cell Signaling), C/EBPα (8178; 1:1,000; Cell Signaling), C/ EBPβ (23,431–1-AP; 1:1,000; Proteintech), tubulin (2146; 1:1,000; Cell Signaling) and both total ERK1/2 and ERK1/2 phosphorylated at Thr202/Tyr204 (1:2,000; Cell Signaling Technology).). Following incubation, the blots were exposed to HRP-conjugated anti-rabbit IgG for a duration of 1 h. The peroxidase activity was subsequently identified utilizing the ECL method (Touch Imager, e-Blot, China).

Immunofluorescence (IF) staining

After 4 h of treatment with forskolin (FSK), KGN cells were fixed in 4% paraformaldehyde for 30 min, permeabilized with 0.1% Triton X-100 for 60 min at 4 °C and blocked with 2% bovine serum albumin (BSA) at room temperature. KGN cells were incubated overnight at 4 °C with anti-FASN antibody (3180; 1:50 dilution; Cell Signaling). After three washes with 2% BSA, KGN cells were incubated with fluorescein isothiocyanate (FITC)-conjugated goat anti-rabbit secondary antibody (2146; 1:20 dilution; Cell Signaling) in the dark at room temperature for 2 h. The nuclei were counterstained with 4′,6-diamidino-2-phenylindole (DAPI) (P0131, Beyotime, China). Images were captured using a confocal microscope

(Olympus, Japan). Additionally, ovarian sections from rats were counterstained with 4',6-diamidino-2-phenylindole (DAPI) (P0131, Beyotime, China). Images were captured using a confocal microscope (Olympus, Japan).

CCK-8 assay

KGN cells from both shNC and shFASN groups were trypsinized and collected for quantification. Subsequently, the cells were distributed into 96-well plates with a density of 3000 cells per well and a total volume of 100μL per well. Each cell group was assigned six wells with the respective compounds and then incubated in a cell incubator. At 6, 24, 48, and 72 h after inoculation, 10 μL of CCK-8 supplement was added to each well and incubated for an additional period of 2 h. Absorbance measurement was performed at a wavelength of 450 nm using an enzyme-linked immunosorbent assay (ELISA) reader and the values were recorded for statistical analysis.

Enzyme-linked immunosorbent assay (ELISA)

Cells from the shNC and shFASN groups were seeded in 12-well plates at a density of $1\times10^{\wedge5}$ cells per well and a volume of 1 mL per well in serum-free medium. After a 24-h starvation period in a cell incubator, cells were then cultured in complete medium for an additional 48 h. The supernatant and serum from rats with local FASN knockdown in the ovaries were collected 4 weeks after lentivirus injection were collected, and then the concentrations of progesterone (MM-51338H2, MEIMIAN, China) and estradiol (MM-0777H2, MEIMIAN, China) in the cultivation medium were quantified using an ELISA method, following the manufacturer's instructions.

Administering ediated vectors into the ovaries of rats

The Ethics Committee of the Animal Center at Wuhan University (WP20230368) authorized all rat trials, which adhered to the NIH criteria for laboratory animal care. Six-week-old Sprague–Dawley rats underwent abdominal surgery to expose the ovaries [14, 15]. Each ovary received two 10uL injections of either shFASN lentivirus (1×10^9 TU/mL) or control ShNC lentivirus (1×10^9 TU/mL), after which the muscle and skin were sutured. 7 days after injection, 6 rats (3 experimental rats and 3 control rats) were euthanized to harvest ovaries. Due to the presence of Green Fluorescent Protein (GFP) in the lentiviral vector system, small ovarian sections were fixed in 4% paraformaldehyde, stained with DAPI, and assessed using a fluorescent microscope to determine the effectiveness of lentiviral transduction. The remaining ovarian tissue was used for RNA and protein extraction to assess FASN expression using qRT-PCR and immunoblotting.

Superovulation

Seven days after lentivirus injection, six 7-week-old rats were intraperitoneally injected with pregnant mare serum gonadotropin (PMSG) (300 IU/kg) (Ninbo sansheng Biological Technology Co.LTD, China) to induce superovulation [16]. This was followed by a human chorionic gonadotropin (hCG) (300 IU/kg) (Ninbo sansheng Biological Technology Co.LTD, China) injection 48 h later, and 16 h after the hCG injection, cumulus-oocyte complexes (COCs) were collected from the oviducts. The COCs were treated with 0.1% hyaluronidase for 5 min to isolate the oocytes. The number of oocytes was recorded and photographed under a microscope.

Assessment of estrous cycle

In the second phase of the animal study, 12 rats were randomly assigned to two groups. The estrous cycle was monitored by examining vaginal cytology for 10 consecutive days [14], starting 3 weeks after lentivirus injection, without superovulation, to evaluate the long-term effects of lentivirus-mediated FASN downregulation in rat ovaries, the flowchart of rat experiments refers to Fig. 3 of Supplementary 1.

Histology

Rat ovaries were fixed in 4% paraformaldehyde and then embedded in paraffin. Pieces of tissue five μm thick were sliced and then soaked in a series of ethanol solutions of varying concentrations to regain moisture. The sections were stained using the hematoxylin–eosin (H&E) method and examined under the microscope.

Statistical analysis

The values are determined by calculating fractions or proportions in relation to negative controls and are then provided as the mean ± SEM. Statistical analysis was performed using ANOVA or unpaired t-tests with GraphPad Prism (version 9.4.0, California). The value of $P<0.05$ was deemed to be statistically significant.

Results

Identification and analysis of DEGs in PCOS

Based on GSE138518, GSE155489, GSE168404 and GSE193123 datasets, the R software package inSilicoMerging was applied to remove batch effects and obtain a new expression matrix (Supplement Fig. 1). Gene expression profiles were obtained from granulosa cells from 15 PCOS patients and 15 controls. We identified 1540 DEGs (1144 upregulated and 396 downregulated) in the merged dataset, adjusted threshold p-value <0.05 and $|\log2\ FC|$ applied >1.0. Hierarchical cluster heatmaps and volcano plot analyses were employed for visualizing the DEGs

(Supplement Fig. 2). These key DEGs serve as a foundation for investigating the pathogenesis of PCOS.

Identification of the common DEGs in PCOS patients and DTH-induced mice

To better investigate the pathogenesis of polycystic ovary syndrome (PCOS), we selected a mouse dataset related to PCOS for our study. From the GSE171431 dataset, we identified 398 DEGs in the ovaries of DHT-induced mice compared to the control group. By intersecting these DEGs with the human combined transcriptome sequencing, we obtained 32 common DEGs (Fig. 2A). Using STRING PPI network analysis, we removed proteins that were not associated with other proteins and obtained 12 hub genes, including FASN/CSL4/PNPLA3/SCARB1/CYP11A1/FABP5/FDPS/GPAM/IDH1/STAR/RAPGEF4/RIMS2. The link sites between each gene and other genes are presented in Fig. 2B and C. The FASN gene was identified as the most prominent candidate, indicating its critical importance in the development of PCOS. The analysis of KEGG disclosed that the DEGs were extremely concentrated in metabolic pathways, ovarian steroidogenesis, fatty acid biosynthesis, and fatty acid metabolism (Fig. 2D). The examination of GO analysis revealed the differences in functions of genes between the PCOS and control groups were primarily associated with enhanced lipid metabolic processes and lipid synthesis processes (Fig. 2E). Overall, these findings suggest that lipid metabolism dysregulation plays a significant role in the dysfunction of granulosa cells in patients with PCOS.

Expression profile of hub genes in PCOS

We collected RNA samples from both PCOS and control patients. Using RT-PCR, we noted a substantial reduction in the expression of FASN and SCARB1 in patients with PCOS ($p < 0.0001$) (Fig. 3A, B) and a significant increase in FABP5, RIMS2 and RAPGEF4 expression ($p < 0.05$) (Fig. 3C-E). The levels of expression of ACSL4, FDPS, GPAM and IDH1 showed no statistically significant differences (Fig. 3F-J). FASN was further investigated due to its significantly reduced expression in PCOS granulosa cells (GCs) and its high number of junctions with other hub genes (Fig. 2C). Furthermore, compared to control patients, the levels of FASN protein were significantly lower in the GCs of PCOS patients ($p < 0.01$) (Fig. 3K). Overall, these results suggest that FASN, a critical gene involved in lipid metabolism, is downregulated in the granulosa cells of patients with PCOS and may play a pivotal role in the onset and progression of the disease.

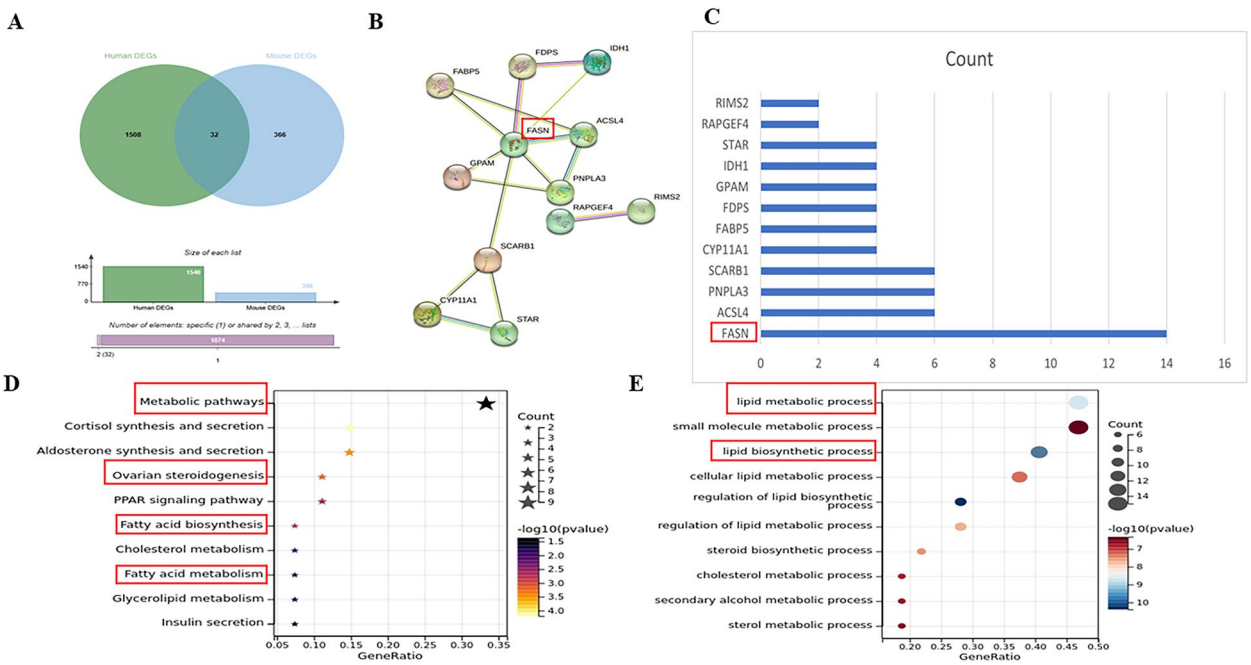

Fig. 2 The overlapping DEGs in PCOS patients and DTH-induced mice. **A** The Venn diagram of human DEGs and mouse DEGs.; **B** The hub genes were identified from the common DEGs by PPI, nodes represent proteins, and edges represent protein–protein interactions; **C** The link sites number of hub genes. **D** The top ten significant KEGG pathways enriched by DEGs; **E** The top ten significant GO terms are enriched by DEGs. In panels D and E, the x-axis represents the Gene Ratio, while the y-axis lists various biological processes or pathways. Larger stars or bubbles indicate a higher number of genes involved in a particular process, and darker colors represent smaller *p*-values, indicating higher statistical significance in the enrichment analysis. The red boxes highlight the key genes, processes, and pathways of interest

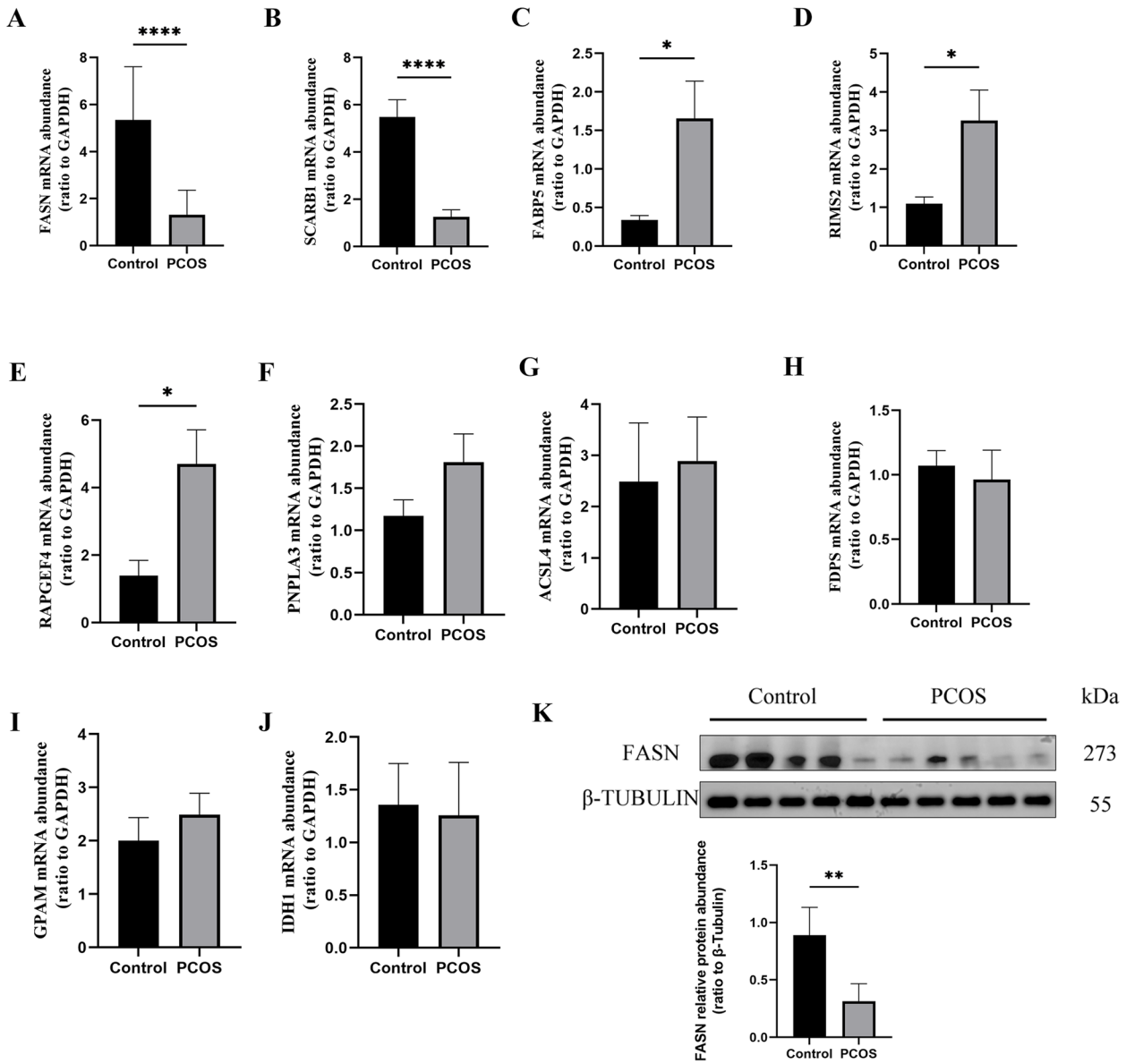

Fig. 3 Expression profile of hub genes in PCOS. **A-J** Hub genes mRNA expression between control group and PCOS patients ($n = 11$ per group). **K** Western blot analysis to quantify the levels of FASN protein in granule cells of both control and PCOS groups ($n = 9$ per group). Data were analyzed by unpaired samples t-test and are expressed as mean ± SEM.*$p < 0.05$, **$p < 0.01$, ****$p < 0.0001$

Knockdown of FASN suppresses KGN cells growth and progesterone secretion, improves estradiol secretion and down regulated ovulation-related genes

With the goal of examining the possible biological role of FASN in KGN cells, we suppressed the expression of FASN using shFASN (Fig. 4A,B). The CCK-8 assay indicated a decline of cellular reproduction ability decreases in KGN cells after the suppression of FASN (Fig. 4C). The FASN downregulation group had elevated estradiol levels (Fig. 4D), but lower the progesterone levels (Fig. 4E).

Because anovulatory infertility is an important feature of PCOS, for the purpose of investigating the probable mechanism of FASN-related signaling pathway molecules in ovulation dysfunction associated with PCOS, we established FASN-depleted and control KGN cells through lentivirus-mediated transfection, confirming the downregulation efficiency at both the mRNA (Fig. 4A) and protein levels (Fig. 4B). The mRNA (Fig. 4F) and protein levels (Fig. 4G) of ovulation-related genes C/EBPα and C/EBPβ are considerably reduced. The results suggest that FASN has a positive influence on the

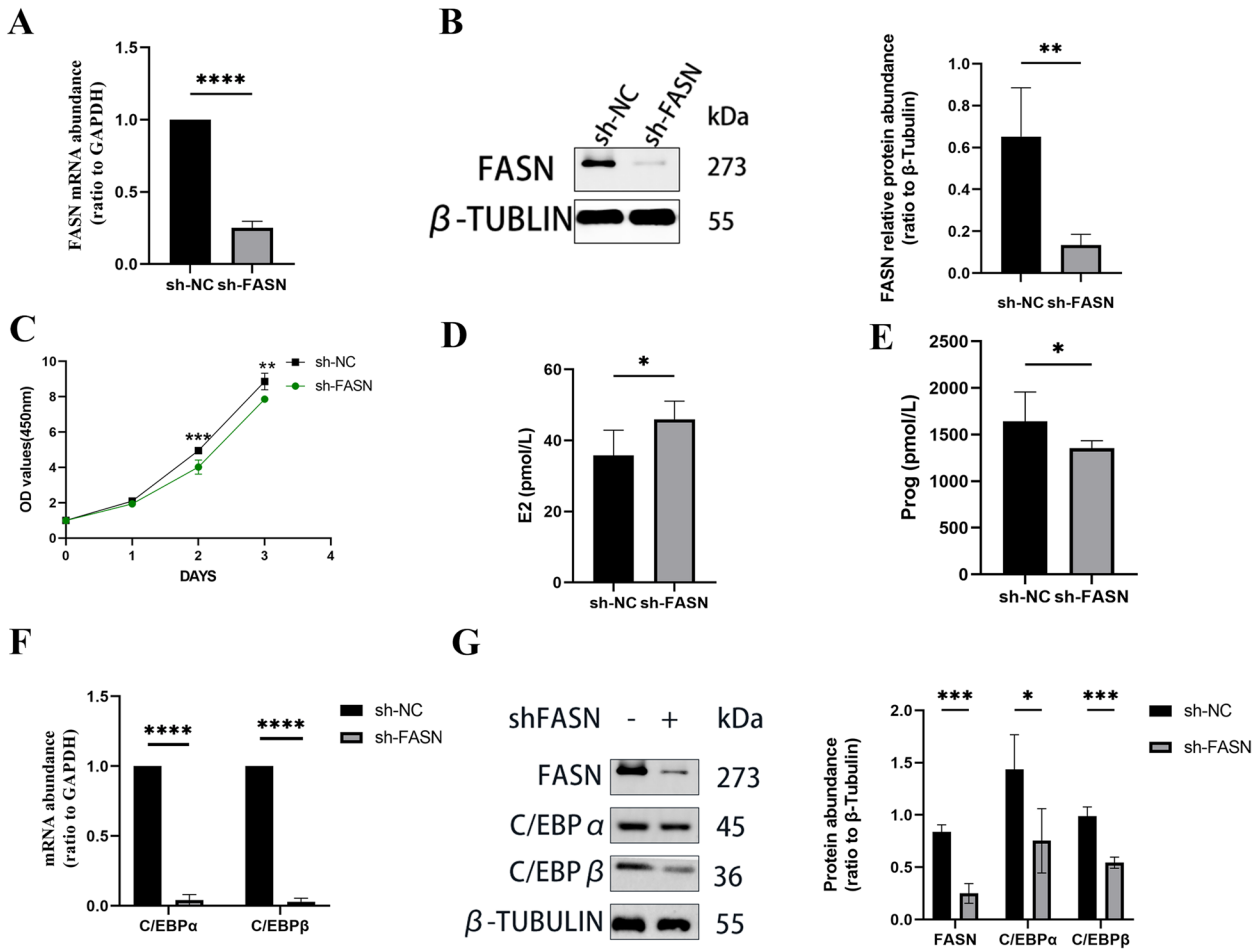

Fig. 4 Effects of FASN knockdown on KGN cells viability, secretion of E2 and P and ovulation-related gene expression **A**, **B**. FASN mRNA and protein expression in KGN cells transfected with sh-NC and sh-FASN. **C** Cell viability was assessed using a CCK-8 assay in KGN cells transfected with sh-NC and sh-FASN. **D** E2 levels in sh-NC and sh-FASN groups were detected by ELISA. **E** P levels in sh-NC and sh-FASN groups were detected by ELISA. **F** mRNA expression of C/EBPα, C/EBPβ after shRNA-mediated FASN knockdown in KGN cells was discovered using qRT-PCR **G** Protein abundance of FASN, C/EBPα, C/EBPβ following the introduction of shFASN lentivirus vectors or control vectors in KGN cells detected by Western blot. Data were analyzed by unpaired samples t-test and are expressed as mean ± SEM from 3–5 experiments. *$p < 0.05$, **$p < 0.01$, ***$p < 0.001$, ****$p < 0.0001$ vs. controls

upregulation of ovulation-related genes, such as C/EBPα and C/EBPβ in granulosa cells.

FASN stimulates ovulation gene expression via the ERK signaling pathway by regulating ERK1/2 activity

Employing forskolin (FSK, 10 mM) to replicate the luteinizing hormone (LH) surge, we triggered the ERK signaling pathway in KGN cells and showed that a crucial time point for LH-induced ovulation is 4 h of FSK treatment [17], which has a positive effect on the mRNA and protein levels of FASN in KGN cells (Fig. 5A,D). Immunofluorescence labeling showed upregulation of FASN expression after 4 h of FSK therapy (Fig. 5G), simultaneously, there was a notable rise in the levels of expression of C/EBPα and C/EBPβ (Fig. 5B-D).

To investigate the role of FASN in the ERK signaling pathway, we observed increased phosphorylation of ERK1/2 after 4 h of FSK treatment, while knockdown of FASN with shFASN significantly reduced ERK1/2 phosphorylation (Fig. 5E). Then, we also pretreated the cells with U0126 (MEK inhibitor, 10 μM) for 1 h, followed by another 4 h of FSK incubation, resulting in effective elimination of LH-induced ERK1/2 Phosphorylation and upregulation of C/EBPβ induced by FSK, with minimal effect on C/EBPα (Fig. 5F).

These results suggest that LH surge triggers FASN surge via ERK signaling, leading to ERK1/2 phosphorylation and promotion of ovulation through upregulation of the ovulation gene C/EBPβ. In PCOS patients, the inhibition of FASN expression in a high-lipid environment

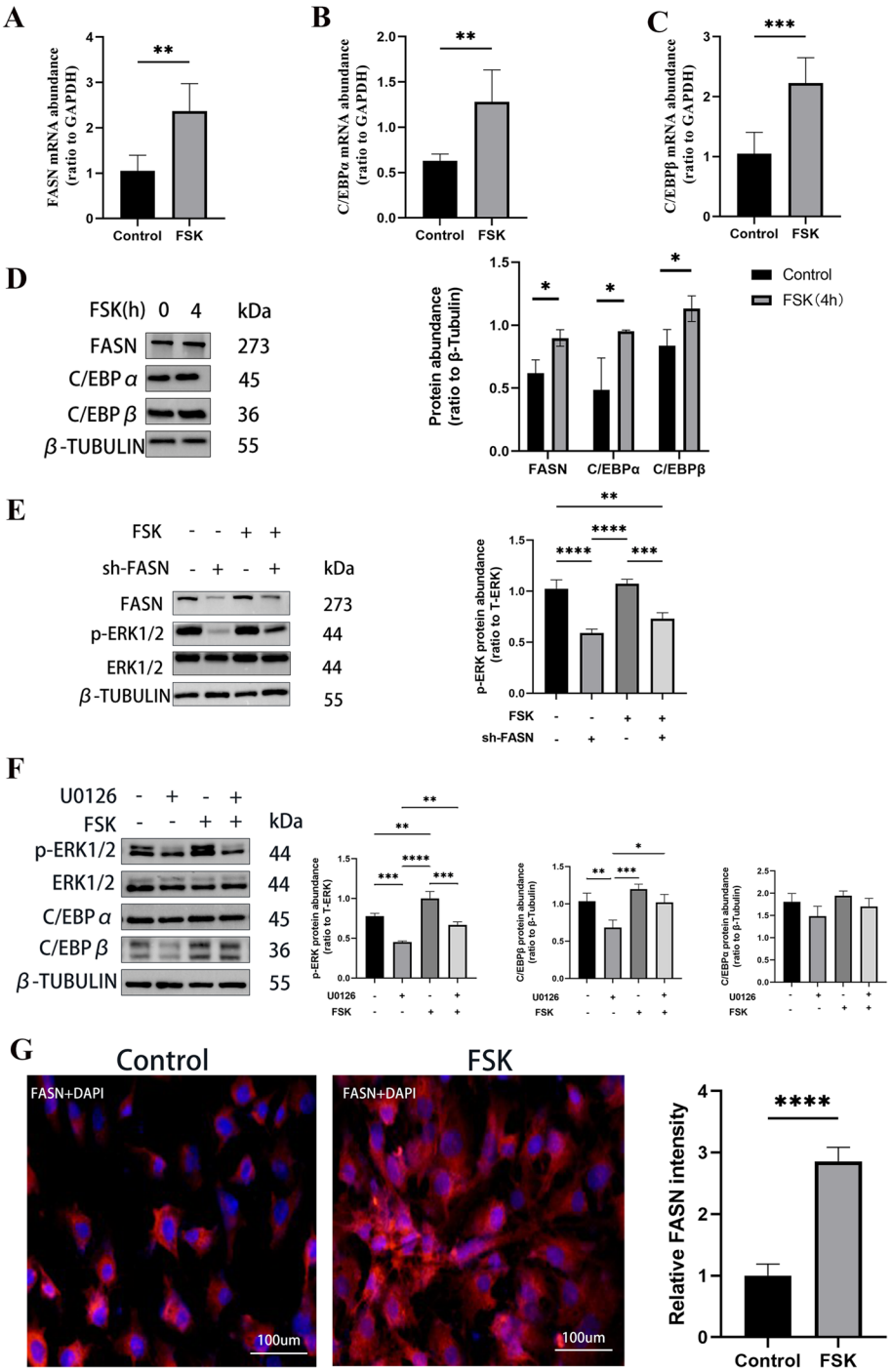

Fig. 5 **A**-**C** Investigation of the impact of FSK (10 uM, 4 h) on the expression of FASN, C/EBPα, and C/EBPβ mRNA in KGN cells. **D** Effects of FSK(10 u M,4 h) on protein levels of FASN, C/EBPα, C/EBPβ in KGN cells. **E** With or without FASN knockdown, the impact of FSK (10 uM, 4 h) on the phosphorylation of ERK1/2 in KGN cells. **F** Effects of FSK (10 uM, 4 h) on ERK1/2 phosphorylation, C/EBPα, C/EBPβ in the presence and absence of inhibitor for ERK1/2 (U0126, 10 uM). **G** KGN cells treated with FSK(10 uM,4 h) were fixed and labelled with anti-FASN antibodies (red). The cellular cores were labeled with 40,6-diamidino-2-phenylindole (DAPI) dye, resulting in a blue coloration. The photomicrographs accurately depict the results of three separate investigations. The analysis of relative fluorescence intensity was conducted using the ImageJ program. The figures display representative blots, data were analyzed using unpaired samples t-test or one-way ANOVA with Tukey's multiple comparison post-hoc test and the results presented are the means ± standard error of the mean (SEM) obtained from 3 to 5 tests. *$P < 0.05$, **$P < 0.01$, ***$P < 0.001$, ****$P < 0.0001$ compared to the control group

suppresses LH-induced ERK1/2 signaling and consequently impairs ovulation.

Ovulation dysfunction in rats induced by downregulation of FASN in ovarian

Our previous studies found that FASN expression is reduced in GCs of PCOS patients and reduced FASN levels could reduce the expression of ovarian gene. To examine the function of FASN in a living organism, we generated a rat model with reduced levels of ovarian FASN by employing lentiviral vectors [14, 15].

One week after lentivirus injection, ovarian samples from three rats per group were analyzed by immunofluorescence and weighing. Green fluorescence was detected in both control and shFASN groups, confirming successful lentivirus delivery without affecting ovarian weight (Fig. 6A, B). The remaining rats received PMSG followed by hCG 48 h later and were euthanized 16 h after hCG ingestion to collect ovarian and oviduct tissues.

Knocking down FASN resulted in a considerable decrease in the quantity of oocytes obtained from the fallopian tubes (Fig. 6D), decreased ERK1/2 phosphorylation, and downregulated the key ovulation genes C/EBPα and C/EBPβ (Fig. 6C). H&E staining 16 h after hCG treatment showed larger antral follicles and less corpora lutea in the shFASN group compared to controls (Fig. 6E). These results suggest that FASN inhibits the expression of key ovulation regulators C/EBPα and C/EBPβ by reducing the phosphorylation of ERK1/2, thereby affecting the final release of the follicle.

Given that one week of FASN downregulation in rat ovaries impairs the super ovulatory response, we explored whether prolonged FASN downregulation could induce PCOS-like phenotypes.

The FASN downregulation group showed no significant differences in body weight (Fig. 7A) but an ovarian weight increase (Fig. 7B, C). Notably, we observed irregular estrous cycles (Fig. 7D) an increase in preantral, small antral, and cystic follicles, along with fewer corpora lutea (Fig. 7F). Serum estradiol levels were increased, and progesterone levels were reduced (Fig. 7E), indicating ovulatory dysfunction. These findings indicate that FASN downregulation following lentivirus injection in rat ovaries results in morphological changes in the ovaries, altered secretion of estrogen and progesterone, and irregular estrous cycles, resembling PCOS-like phenotypes.

Discussion

The pathogenesis of PCOS remains largely unknown [18–21]. Those patients experience a delay in the follicles' late development, called the sinus follicular phase, which results in the follicles not growing properly [2]. This ultimately hinders ovulation [22]. The GCs in the follicles have a vital part in oocyte advancement and ovulation [3].

To identify the key genes involved in the development and progression of PCOS, we identified 32 common differential genes of granulosa cells in both PCOS patients and a DHT-induced animal model ovary. KEGG analysis revealed enrichment in metabolic pathways, ovarian steroidogenesis, and fatty acid biosynthesis and metabolism. GO analysis demonstrated substantial enhancement in lipid metabolic processes. As the post study have express that granulosa cell lipid metabolism is crucial for oocyte development [23], and abnormalities in this process are associated with PCOS [24]. Dyslipidemia's frequency is high in anovulatory PCOS patients (41.3%−70%), characterized by elevated serum cholesterol and triglyceride concentrations, elevated low-density lipoprotein (LDL) concentrations, and reduced high-density lipoprotein (HDL) concentrations [25]. Within the blood and follicle fluid of individuals with PCOS patients, the fatty acid profiles are considerably different from those of women in good health [26]. Upregulation of the NKB-NK3R system and MAPK-ERK signaling pathway in KGN cells can be induced by palmitic acid supplementation to mimic the lipid-rich environment of PCOS cells. Within the ovaries tissues, there is an increased expression of the NKB-NK3R system in PCOS-like mice leading to apparent ovulation disruption, insufficient progesterone levels, and an inflammatory state [27]. Disturbed lipid metabolism in granulosa cells is induces cell death or autophagy [28], which subsequently leads to ovulation disorder, suggesting that lipid metabolism disorders in GCs may be associated with the occurrence of PCOS [29].

Through STRING protein network analysis, we identified 12 hub genes, which were validated in granulosa cells of PCOS patients. FASN was ultimately selected for further investigation. FASN, a central enzyme for de novo lipogenesis, is a key gene involved in lipid synthesis and metabolism [30–32]. Our analysis of GEO database information indicated that FASN expression decreases in GCs from both PCOS patients and DHT-induced models, a finding confirmed in GCs from PCOS patients [33]. In vitro, suppression of FASN expression inhibited KGN cell proliferation, increased estradiol secretion, and decreased progesterone secretion. These findings align with prior research on GCs from other species [34].

Some studies have shown that FASN is present in follicular granulosa cells of goose and significantly influences follicular maturation and steroidogenesis. Overexpressed FASN increased the apoptosis of GCs, furthermore, the interference with FASN resulted in a decrease in their progesterone synthesis in goose GCs by suppressing the the manifestation of steroidogenic acute regulatory protein (STAR) [34, 35]. When culturing bovine granulosa

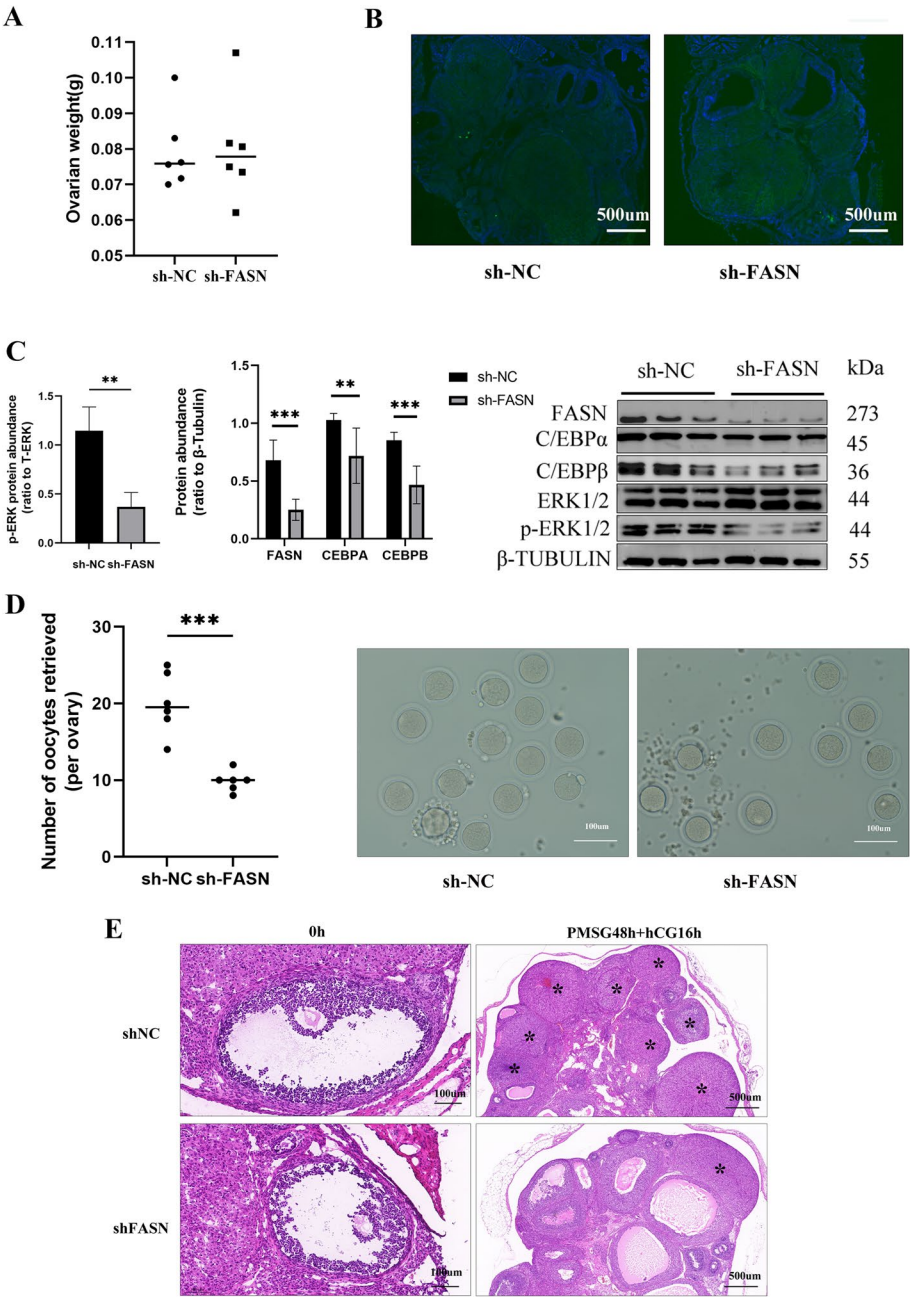

Fig. 6 Lentivirus vectors promote downregulation of FASN, leading to ovulatory failure in rats. **A** Ovarian weight of rats before superovulation ($n=6$ per group). **B** Ovarian sections were frozen before superovulation. Cell nuclei were stained with 4′,6-diamidino-2-phenylindole (DAPI) (blue). Lentivirus showed green fluorescence that could be seen by means of a fluorescent scope.The photomicrographs were typical of those found in three separate studies. **C** hCG16h, protein levels of FASN, C/EBPα, C/EBPβand ERK1/2 phosphorylation was examined in ovaries from two groups($n=3$ per group). **D** Oocytes numbers per ovary ($n=6$ for every group). **E** Rats injected with the control vector (top) and the FASN-lentivirus vector (bottom) showed different ovarian morphologies had distinct ovarian morphologies after superovulation (PMSG48h + hCG16 h).The asterisk indicates the corpus luteum. Scale bar: 500 m. Data were analyzed using unpaired samples t-test and are presented as mean ± SEM. $^{*}P<0.05$, $^{**}P<0.01$, $^{***}P<0.001$ vs. the control group

cells in the laboratory, the use of C75 to inhibit FASN resulted in a reduction in progesterone production by blocking cholesterol synthesis. In addition, it slowed cell growth by reducing the expression of cyclin D2 [36]. In addition, the introduction of palmitic acid hindered the growth of bovine GCs by triggering programmed cell

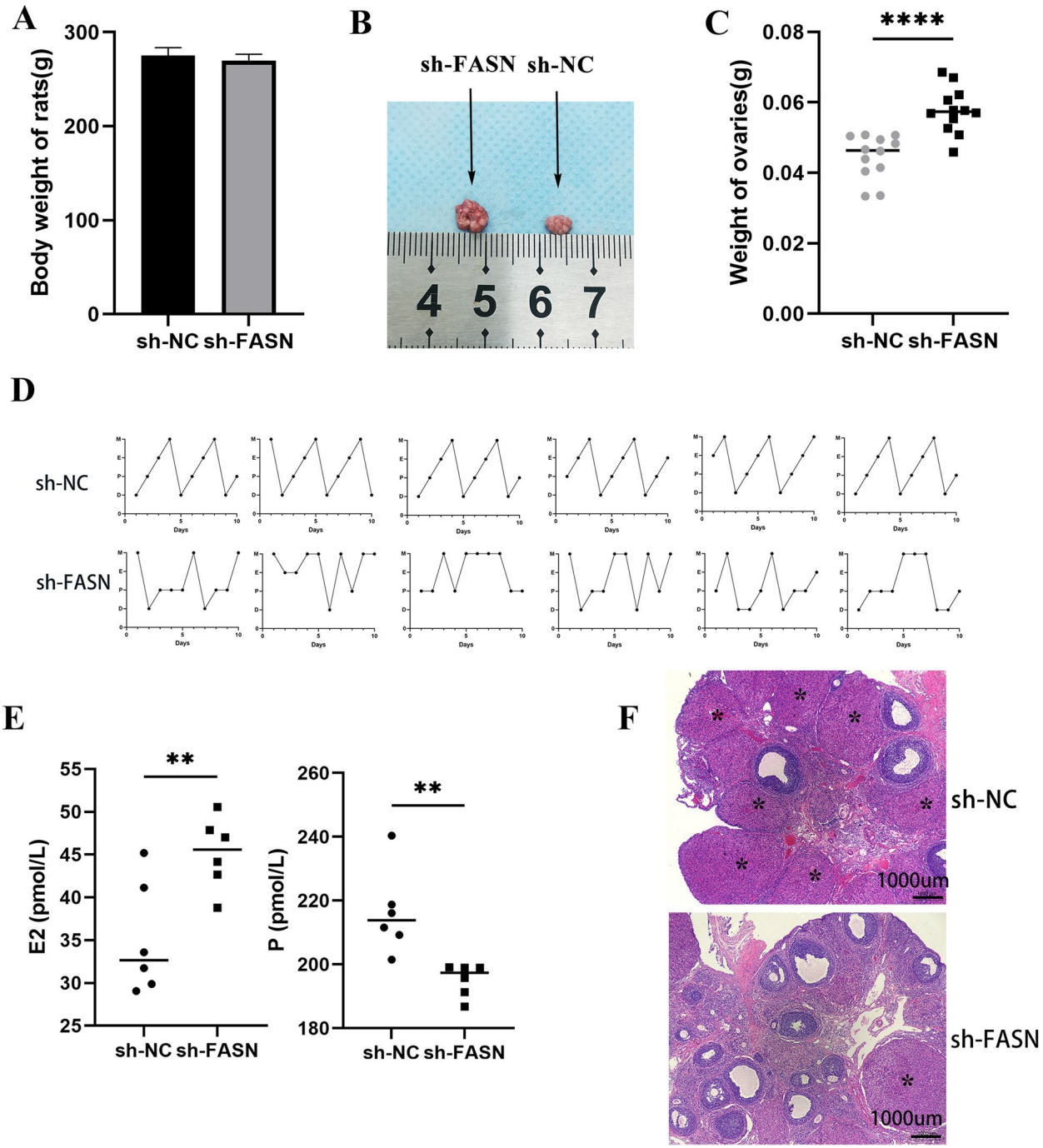

Fig. 7 Effects of 4-week FASN downexpression in rat ovaries mediated by lentivirus vectors. **A** Body weight of rats($n=6$ per group); **B** Appearance of the rat ovaries; **C** Weight of rats($n=12$ per group); **D** Estrous cycles were detected in rats injected with control vector (above) or FASN lentivirus vector (below)($n=6$ per group); **E** Serum estradiol(E2)(left) and Progesterone(right) levels detected by ELISA analysis($n=6$ per group); **F** Ovarian morphology of rats injected with control vector (above) or FASN lentivirus vector (below). Asterisk stands for corpus luteum. Scale bar, 1000 μm. Data were analyzed using unpaired samples t-test and are presented as mean ± SEM. $^{*}P<0.05$, $^{**}P<0.01$, $^{**}P<0.001$ vs. the control group

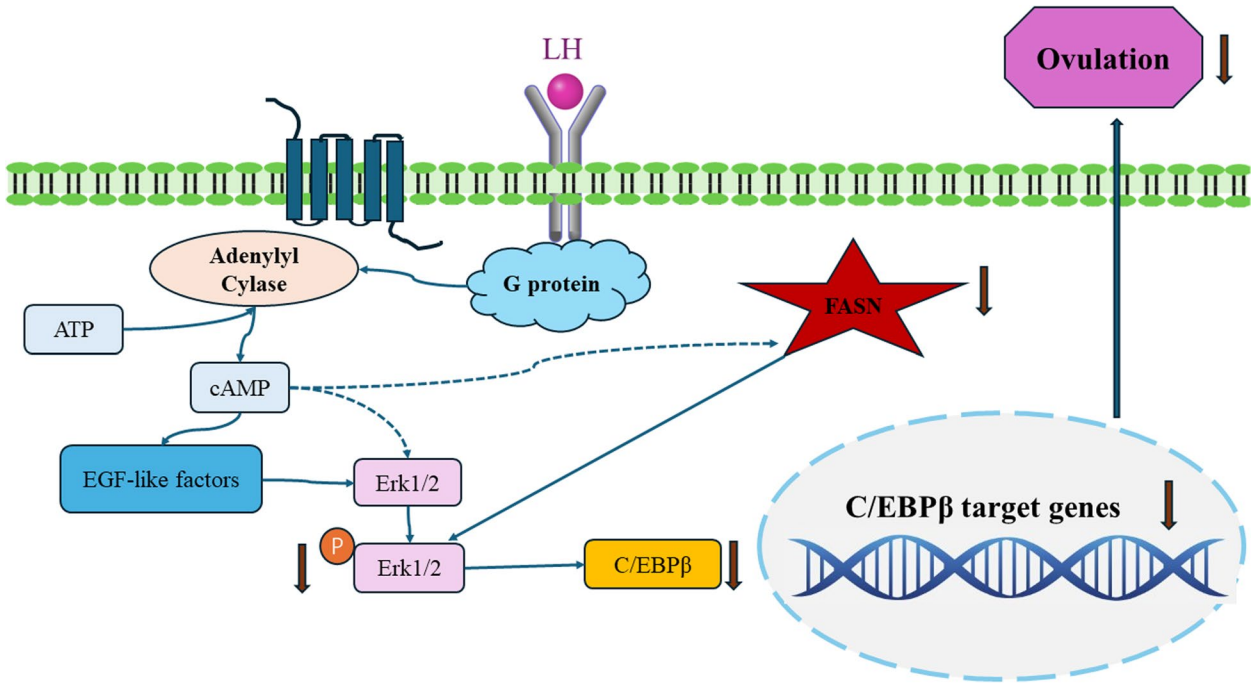

Fig. 8 All ovulation events are triggered by an LH surge, engaged in oocyte maturation, cumulus expansion, and follicle rupture. Downregulation of FASN expression in PCOS results in block of ovulation by ERK1/2 phosphorylation, hence suppressing C/EBPβ and other ovulatory genes

death and promoted the production of estradiol-17 (E2) by activating NADPH-dependent enzymes in the ovarian aromatase enzyme complex.

Furthermore, we focused on the role of FASN in ovulation. In vitro experiments revealed LH surge-induced upregulation of FASN, indicating that FASN might have a pivotal function in controlling the ovulation. The results of our research indicated a decrease in expression of FASN can reduce the transcription of the ovulation-associated genes C/EBPα and C/EBPβ. Previous studies have shown that mice lacking C/EBPβ exhibit reduced fertility, impaired expansion of the COC, and lack of luteinization, leading to ovulation dysfunction. While C/EBPα^{-}deficient mice have regular fertility, the double mutants C/EBPα/β$^{gc-/-}$ lacking are unable to ovulate [10].

In KGN cells, downregulation of FASN inhibited ERK1/2 phosphorylation signaling, thereby downregulating the expression of downstream C/EBPα and C/EBPβ. Prior research indicated that ERK1/2 [9, 37] regulates the display of numerous genes that are quickly activated due to the LH spike [38] within 4 h in GCs found in follicles that are about to ovulate. Our investigation found that pretreatment use of the ERK signaling inhibitor U0126 [39] successfully eliminated the increase in C/EBP caused by forskolin-mimicking LH surge. We discovered that FASN is essential in the process of ERK1/2 phosphorylation during ovulation caused by the LH surge. Decreased expression of FASN in the GCs of patients with PCOS has implications for regular ovulation triggered by the LH surge.

To conduct a more in-depth examination of the function of FASN in the ovulation process, FASN was downregulated in rat ovaries by injecting lentivirus. For this research, we observed that reducing rodent ovaries FASN expression inhibited the expression of genes associated with ovulation, comprising phosphorylated ERK1/2, C/EBPα, and C/EBPβ. This inhibition affected granulosa cell proliferation, follicular development, oocyte maturing, and follicular disruption. One week after downregulation of FASN expression and induction of ovulation, the ovulation rate decreased significantly in rats with reduced FASN expression accompanied by reduced luteinization. Results highlight the central role of FASN in studying the mechanism of ovulation and determining the underlying molecular signaling pathways.

We examined the activity of FASN, a crucial molecule in lipid metabolism, in relation to granulosa cell proliferation, secretion of estradiol and progesterone, and its influence on ovulation dysfunction in PCOS (Fig. 8). Previous studies have also shown that under the influence of hyperandrogenism and dyslipidemia, several genes involved in fatty acid synthesis, such as fatty acid desaturase genes 2(FADS2) [40]、stearoyl coA desaturase(SCD)

and FASN, are downregulated in the granulosa cells of PCOS patients [33]. This downregulation may affect fatty acid and cholesterol synthesis within the granulosa cells, ultimately influencing follicular development [41]. However, the exact mechanisms remain unclear. In the present study, we confirmed that FASN expression is reduced in granulosa cells and that this downregulation impacts the expression of ovulation-related genes, C/EBPα and C/EBPβ, through the modulation of ERK1/2 phosphorylation, thereby affecting ovulation. These findings indicated that FASN could serve as a potential molecular target for treating PCOS-related ovulatory dysfunction. Targeting the upregulation of FASN expression in granulosa cells may offer a novel therapeutic approach. Furthermore, we can investigate the potential of enhancing oocyte maturation by upregulating FASN expression in granulosa cells during in vitro follicle culture. However, further experiments are required to validate this hypothesis. The results of our study confirm the involvement of FASN in ovulation disorders associated with PCOS, provide new perspectives on the processes of anovulation and provide a biological basis for possible therapeutic interventions to improve ovulation in PCOS patients.

Despite extensive literature search and bioinformatics analysis, our investigation has numerous limitations. Firstly, the limited accessibility of available data and the heterogeneity of studies presented challenges. Genes exploited in our integrative investigation were diagnosed through a literature survey that focused on heterogeneous studies with poor overlap in molecular signatures characterizing standard or affected granulosa cells. The selection of these datasets may introduce bias, particularly as the four PCOS datasets, comprising data from 15 PCOS and control patients, may not fully capture the heterogeneity of the PCOS population. Variations in genetic, hormonal, and environmental factors can influence the clinical presentation of PCOS, and these datasets may not encompass this diversity. Moreover, the absence of data on baseline BMI and lipid levels introduces the possibility that these factors may have influenced the results. Additionally, the single DHT-induced mouse model dataset may not fully replicate the complex biological mechanisms underlying human PCOS. To address these limitations, future studies should include a broader range of datasets, incorporating data from different ethnic groups and clinical subtypes of PCOS, to enhance the generalizability of the findings. Secondly, our prioritization of selected genes may have limited our findings. While 12 candidate genes were selected for expression analysis, most of the genes were not utilized for validation. Then, the tiny size of both the PCOS and control groups may have decreased the statistical power of our study. And lastly, previous research found increased fatty acids in PCOS granulosa cells [26], but the interaction between fatty acids and FASN in the granulosa cells, as a fatty acid synthase, has not been specifically studied. Further investigations are warranted to explore the influence of dyslipidemia on FASN expression in ovarian granulosa cells of PCOS patients, as well as its potential association with ovulation disorders in PCOS. While our data suggests an association between FASN downregulation and ovulatory dysfunction in PCOS, the nature of this relationship—whether causal or merely correlational—remains unclear. To establish causality, longitudinal studies and experimental interventions targeting FASN across various PCOS models are necessary. Additionally, it will be crucial to monitor changes in FASN expression over time in PCOS patients and correlate these changes with the onset and progression of ovulatory dysfunction. Moreover, due to the high molecular weight of FASN (273 kDa), developing a model for FASN overexpression is currently not feasible. No effective method for replacing FASN has been identified as a potential therapeutic approach, which represents an important avenue for future research.

Conclusions

In conclusion, using public databases and several computational algorithms, we were able to identify FASN as a central hub gene in the GCs of women with PCOS. Our in vitro analysis confirmed that FASN is a reliable predictive marker and regulator of the steroidogenic process. Our data suggested that FASN plays a significant role in the development of ovulation disorder in PCOS, as its downregulation may inhibit ovulation by targeting the ERK signaling pathway (Fig. 8). Therefore, improving FASN expression in GCs of PCOS patients coupled with assisted reproductive technology (ART) could serve as a potentially effective biological approach to treat ovulation disorders in PCOS. Future studies will verify the causal link between FASN and ovulatory dysfunction in PCOS by increasing sample size and species diversity. We will also explore methods to enhance FASN expression in granulosa cells to improve follicular maturation and restore normal ovulation in PCOS patients.

Abbreviations

PCOS	Polycystic ovary syndrome
GCs	Granulosa cells
DHT	Dihydrotestosterone
GEO	Gene Expression Omnibus
DEGs	Differentially expressed genes
PPI	Protein-protein interaction
GO	Gene Ontology
KEGG	Kyoto Encyclopedia of Genes and Genomes
IVF	In vitro fertilization
FSK	Forskolin
qRT-PCR	quantitative real-time polymerase chain reaction
GFP	Green fluorescent protein
IF	Immunofluorescence

ELISA	Enzyme-linked immunosorbent assay
COCs	Cumulus-oocyte complexes
H&E	Hematoxylin and eosin
ART	Assisted reproductive technology

Supplementary Information

The online version contains supplementary material available at https://doi.org/10.1186/s13048-025-01645-y.

Supplementary Material 1.

Supplementary Material 2.

Acknowledgements
We thank the support of the clinical and laboratory teams in data collection and statistical analyses.

Clinical trial number
Not applicable.

Authors' contributions
Zhaoping Tan conceived, planned the tests and performed the experiments and analyzed the data of the work. Tiancheng Wu, Liang Chen and Yating Li helped to finish the experiments. Lili Sun and Ming Zhang helped to the collection clinical specimens. Mei Wang helped to revise the manuscript. Yuanzhen Zhang and Lili Sun supervised and reviewed the manuscript. All authors read and approved the final manuscript.

Funding
The work was financially supported by the Natural Science Foundation of Hubei Province (2022CFC023) and the Huanggang Special Project, Hubei Province at the relevant level for scientific and technological innovation (YBXM20230040), the Medical Science and Technology Innovation Platform Project of Wuhan University Zhongnan Hospital (PTXM2023030), supports surface of Zhongnan Hospital of Wuhan University, 2023 Medical Science and Technology Innovation Platform Support Project (PTXM2023030), Hubei Provincial Health Commission Traditional Chinese Medicine Administration Project(ZX-KYXM2024012) and Zhongnan Hospital of Wuhan University Innovation Cultivation Fund(CXPY2024084).

Data availability
No datasets were generated or analysed during the current study.

Declarations

Ethics approval and consent to participate
This study was carefully reviewed and approved by the Ethics Committee of Zhongnan Hospital of Wuhan University (Number: 2021136 K). All procedures performed in studies were in accordance with the ethical standards of Ethics Committee of Zhongnan Hospital of Wuhan University with the Declaration of Helsinki.

Consent for publication
Not applicable.

Competing interests
The authors declare no competing interests.

Received: 24 July 2024 Accepted: 12 March 2025
Published online: 01 April 2025

References

1. Joham AE, Norman RJ, Stener-Victorin E, Legro RS, Franks S, Moran LJ, Boyle J, Teede HJ. Polycystic ovary syndrome. Lancet Diabetes Endocrinol. 2022;10:668–80. https://doi.org/10.1016/S2213-8587(22)00163-2.
2. Stener-Victorin E, Teede H, Norman RJ, Legro R, Goodarzi MO, Dokras A, Laven J, Hoeger K, Piltonen TT. Polycystic ovary syndrome Nat Rev Dis Primers. 2024;10:27. https://doi.org/10.1038/s41572-024-00511-3.
3. Escobar-Morreale HF. Polycystic ovary syndrome: definition, aetiology, diagnosis and treatment. Nat Rev Endocrinol. 2018;14:270–84. https://doi.org/10.1038/nrendo.2018.24.
4. Gorry A, White DM, Franks S. Infertility in polycystic ovary syndrome: focus on low-dose gonadotropin treatment. Endocrine. 2006;30:27–33. https://doi.org/10.1385/endo:30:1:27.
5. Zhang Q, Ren J, Wang F, Pan M, Cui L, Li M, Qu F. Mitochondrial and glucose metabolic dysfunctions in granulosa cells induce impaired oocytes of polycystic ovary syndrome through Sirtuin 3. Free Radic Biol Med. 2022;187:1–16. https://doi.org/10.1016/j.freeradbiomed.2022.05.010.
6. Munakata Y, Kawahara-Miki R, Shiratsuki S, Tasaki H, Itami N, Shirasuna K, Kuwayama T, Iwata H. Gene expression patterns in granulosa cells and oocytes at various stages of follicle development as well as in in vitro grown oocyte-and-granulosa cell complexes. Reprod Dev. 2016;62:359–66. https://doi.org/10.1262/jrd.2016-022.
7. Pierre A, Taieb J, Giton F, Grynberg M, Touleimat S, El Hachem H, Fanchin R, Monniaux D, Cohen-Tannoudji J, di Clemente N, Racine C. Dysregulation of the Anti-Mullerian Hormone System by Steroids in Women With Polycystic Ovary Syndrome. J Clin Endocrinol Metab. 2017;102:3970–8. https://doi.org/10.1210/jc.2017-00308.
8. Richards JS, Ascoli M. Endocrine, Paracrine, and Autocrine Signaling Pathways That Regulate Ovulation. Trends In Endocrinology and Metabolism: TEM. 2018;29:313–25. https://doi.org/10.1016/j.tem.2018.02.012.
9. Fan H-Y, Liu Z, Shimada M, Sterneck E, Johnson PF, Hedrick SM, Richards JS. MAPK3/1 (ERK1/2) in ovarian granulosa cells are essential for female fertility. Science (New York, NY). 2009;324:938–41. https://doi.org/10.1126/science.1171396.
10. Fan H-Y, Liu Z, Johnson PF, Richards JS. CCAAT/Enhancer-Binding Proteins (C/EBP)-α and -β Are Essential for Ovulation, Luteinization, and the Expression of Key Target Genes. MolEndocrinol. 2011;25:253–68. https://doi.org/10.1210/me.2010-0318.
11. Caldwell ASL, Middleton LJ, Jimenez M, Desai R, McMahon AC, Allan CM, Handelsman DJ, Walters KA. Characterization of reproductive, metabolic, and endocrine features of polycystic ovary syndrome in female hyperandrogenic mouse models. Endocrinol. 2014;155:3146–59. https://doi.org/10.1210/en.2014-1196.
12. Shen W, Song Z, Zhong X, Huang M, Shen D, Gao P, Qian X, Wang M, He X, Wang T, et al. Sangerbox: a comprehensive, interaction-friendly clinical bioinformatics analysis platform. iMeta. 2022;1:e36. https://doi.org/10.1002/imt2.36.
13. Ritchie ME, Phipson B, Wu D, Hu Y, Law CW, Shi W, Smyth GK. limma powers differential expression analyses for RNA-sequencing and microarray studies. Nucleic Acids Res. 2015;43:e47. https://doi.org/10.1093/nar/gkv007.
14. Zhou R, Li S, Liu J, Wu H, Yao G, Sun Y, Chen ZJ, Li W, Du Y. Up-regulated FHL2 inhibits ovulation through interacting with androgen receptor and ERK1/2 in polycystic ovary syndrome. EBioMedicine. 2020;52:102635. https://doi.org/10.1016/j.ebiom.2020.102635.
15. Di F, Liu J, Li S, Yao G, Hong Y, Chen ZJ, Li W, Du Y. ATF4 Contributes to Ovulation via Regulating COX2/PGE2 Expression: A Potential Role of ATF4 in PCOS. Front Endocrinol (Lausanne). 2018;9:669. https://doi.org/10.3389/fendo.2018.00669.
16. Popova E, Krivokharchenko A, Ganten D, Bader M. Comparison between PMSG- and FSH-induced superovulation for the generation of transgenic rats. Mol Reprod Dev. 2002;63:177–82. https://doi.org/10.1002/mrd.10173.
17. Shimada M, Hernandez-Gonzalez I, Gonzalez-Robayna I, Richards JS. Paracrine and Autocrine Regulation of Epidermal Growth Factor-Like Factors in Cumulus Oocyte Complexes and Granulosa Cells: Key Roles for Prostaglandin Synthase 2 and Progesterone Receptor. Mol Endocrinol. 2006;20:1352–65. https://doi.org/10.1210/me.2005-0504.
18. Goodarzi MO, Dumesic DA, Chazenbalk G, Azziz R. Polycystic ovary syndrome: etiology, pathogenesis and diagnosis. Nat Rev Endocrinol. 2011;7:219–31. https://doi.org/10.1038/nrendo.2010.217.
19. Azziz R, Carmina E, Chen Z, Dunaif A, Laven JSE, Legro RS, Lizneva D, Natterson-Horowtiz B, Teede HJ, Yildiz BO. Polycystic ovary syndrome. Nat Rev Dis Primers. 2016;2:16057. https://doi.org/10.1038/nrdp.2016.57.

20. Revised, consensus on diagnostic criteria and long-term health risks related to polycystic ovary syndrome (PCOS). Human Reproduction (Oxford, England). 2003;2004(19):41–7. https://doi.org/10.1016/j.fertnstert.2003.10.004.
21. Group TREA-SPCW: Revised. consensus on diagnostic criteria and long-term health risks related to polycystic ovary syndrome. Fertil Steril. 2003;2004(81):19–25. https://doi.org/10.1016/j.fertnstert.2003.10.004.
22. Adams JM, Taylor AE, Crowley WF, Hall JE. Polycystic ovarian morphology with regular ovulatory cycles: insights into the pathophysiology of polycystic ovarian syndrome. J Clin Endocrinol Metab. 2004;89:4343–50. https://doi.org/10.1210/jc.2003-031600.
23. Liu T, Qu J, Tian M, Yang R, Song X, Li R, Yan J, Qiao J: Lipid Metabolic Process Involved in Oocyte Maturation During Folliculogenesis. Front Cell Dev Biol 2022, 10. https://doi.org/10.3389/fcell.2022.806890.
24. Zhang CH, Liu XY, Wang J: Essential Role of Granulosa Cell Glucose and Lipid Metabolism on Oocytes and the Potential Metabolic Imbalance in Polycystic Ovary Syndrome. Int J Mol Sci 2023, 24. https://doi.org/10.3390/ijms242216247.
25. Zhang J, Fan P, Liu H, Bai H, Wang Y, Zhang F. Apolipoprotein A-I and B levels, dyslipidemia and metabolic syndrome in south-west Chinese women with PCOS. Hum Reprod. 2012;27:2484–93. https://doi.org/10.1093/humrep/des191.
26. Lai Y, Ye Z, Mu L, Zhang Y, Long X, Zhang C, Li R, Zhao Y, Qiao J. Elevated Levels of Follicular Fatty Acids Induce Ovarian Inflammation via ERK1/2 and Inflammasome Activation in PCOS. J Clin Endocrinol Metab. 2022;107:2307–17. https://doi.org/10.1210/clinem/dgac281.
27. Guo F, Fernando T, Zhu X, Shi Y. The overexpression of neurokinin B–neurokinin 3 receptor system exerts direct effects on the ovary under PCOS-like conditions to interfere with mitochondrial function. Am J Reprod Immunol. 2022;89. https://doi.org/10.1111/aji.13663.
28. Esmaeilian Y, Hela F, Bildik G, İltumur E, Yusufoglu S, Yildiz CS, Yakin K, Kordan Y, Oktem O. Autophagy regulates sex steroid hormone synthesis through lysosomal degradation of lipid droplets in human ovary and testis. Cell Death Dis. 2023;14:342. https://doi.org/10.1038/s41419-023-05864-3.
29. Schube U, Nowicki M, Jogschies P, Blumenauer V, Bechmann I, Serke H. Resveratrol and desferoxamine protect human OxLDL-treated granulosa cell subtypes from degeneration. J Clin Endocrinol Metab. 2014;99:229–39. https://doi.org/10.1210/jc.2013-2692.
30. Levate G, Wang Y, McCredie R, Fenwick M, Rae MT, Duncan WC, Siemienowicz KJ. Insights into the effects of sex and tissue location on the evolution of adipocyte dysfunction in an ovine model of polycystic ovary syndrome (PCOS). Mol Cell Endocrinol. 2025;595:112416. https://doi.org/10.1016/j.mce.2024.112416.
31. Choi W, Li C, Chen Y, Wang Y, Cheng Y: Structural dynamics of human fatty acid synthase in the condensing cycle. Nature 2025:1–3. https://doi.org/10.1038/s41586-025-08782-w.
32. Schultz K, Costa-Pinheiro P, Gardner L, Pinheiro LV, Ramirez-Solis J, Gardner SM, Wellen KE, Marmorstein R: Snapshots of acyl carrier protein shuttling in human fatty acid synthase. Nature 2025:1–9. https://doi.org/10.1038/s41586-025-08587-x.
33. Liao B, Qi X, Yun C, Qiao J, Pang Y. Effects of Androgen Excess-Related Metabolic Disturbances on Granulosa Cell Function and Follicular Development. Front Endocrinol. 2022;13:815968. https://doi.org/10.3389/fendo.2022.815968.
34. Chen X, Huang K, Hu S, Lan G, Gan X, Gao S, Deng Y, Hu J, Li L, Hu B, et al. FASN-Mediated Lipid Metabolism Regulates Goose Granulosa Cells Apoptosis and Steroidogenesis. Front Physiol. 2020;11:600. https://doi.org/10.3389/fphys.2020.00600.
35. Wen R, Gan X, Hu S, Gao S, Deng Y, Qiu J, Sun W, Li L, Han C, Hu J, Wang J. Evidence for the existence of de novo lipogenesis in goose granulosa cells. Poult Sci. 2019;98:1023–30. https://doi.org/10.3382/ps/pey400.
36. Elis S, Desmarchais A, Maillard V, Uzbekova S, Monget P, Dupont J. Cell proliferation and progesterone synthesis depend on lipid metabolism in bovine granulosa cells. Theriogenology. 2015;83:840–53. https://doi.org/10.1016/j.theriogenology.2014.11.019.
37. Xi G, An L, Wang W, Hao J, Yang Q, Ma L, Lu J, Wang Y, Wang W, Zhao W, et al. The mRNA-destabilizing protein Tristetraprolin targets "meiosis arrester" Nppc mRNA in mammalian preovulatory follicles. Proc Natl Acad Sci U S A. 2021;118. https://doi.org/10.1073/pnas.2018345118.
38. Singh S, Kaur M, Thapar P, Kaur A: Genetic association between LHCGR variants and polycystic ovary syndrome: a meta-analysis. J Ass Reprod Genet 2025,24. https://doi.org/10.1007/s10815-025-03434-4.
39. Lee J, Stanley JA, McCracken JA, Banu SK, Arosh JA. Intrauterine coadministration of ERK1/2 inhibitor U0126 inhibits interferon TAU action in the endometrium and restores luteolytic PGF2alpha pulses in sheep. Biol Reprod. 2014;91:46. https://doi.org/10.1095/biolreprod.113.111872.
40. Tian Y, Zhang W, Zhao S, Sun Y, Bian Y, Chen T, Du Y, Zhang J, Wang Z, Huang T, et al. FADS1-FADS2 gene cluster confers risk to polycystic ovary syndrome. Sci Rep. 2016;6:21195. https://doi.org/10.1038/srep21195.
41. Shi M, Sirard MA. Metabolism of fatty acids in follicular cells, oocytes, and blastocysts. Reprod Fertil. 2022;3:R96–108. https://doi.org/10.1530/RAF-21-0123.

Publisher's Note